

Abundance determinations in extragalactic H II regions

*L. S. Pilyugin**

Main Astronomical Observatory of NAS of Ukraine, 27 Akademika Zabolotnoho St., 03680 Kyiv, Ukraine

The abundance determinations in extragalactic H II regions are reviewed. The discussion is mainly focused on the different variants of the strong line method (calibrations). However, we do not list and consider in details a numerous relations suggested to convert metallicity-sensitive emission-line combinations into metallicity or temperature estimates. Instead we analyse the foundations of different types of calibrations and problems which those calibrations encounter. The empirical (defined by the H II regions with well-measured abundances) and theoretical or model (defined by the set of photoionization models of H II regions) metallicity scales are discussed.

Key words: galaxies abundances, ISM abundances, H II regions

INTRODUCTION

Accurate metallicities play a key role in many investigations of galaxies. Gas-phase oxygen and nitrogen abundances are broadly used to measure these metallicities. It is believed (e.g. [58]) that emission lines due to photoionization by massive stars are the most powerful indicator of the chemical composition of galaxies, both in the low- and intermediate-redshift universe. Accurate oxygen and nitrogen abundances in H II regions can be derived via the classic T_e method, often referred to as the direct method. This method is based on the measurements of the electron temperature t_3 within the [O III] zone and/or the electron temperature t_2 within the [O II] zone. The ratio of the nebular to auroral oxygen line intensities $[O III](\lambda 4959 + \lambda 5007)/[O III]\lambda 4363$ is usually used for the t_3 determination, while the ratios of the nebular to auroral nitrogen line intensities $[N II](\lambda 6548 + \lambda 6584)/[N II]\lambda 5755$ or oxygen line intensities $[O II](\lambda 3727 + \lambda 3729)/[O II](\lambda 7320 + \lambda 7330)$ are used for the t_2 determination. In high-metallicity H II regions, however, the auroral lines become too faint to be detected.

Some combinations of the strong nebular line intensities in spectra of H II regions can be calibrated in terms of their oxygen abundances. This approach to abundance determinations in H II regions, first suggested by Pagel et al. (1979) [33] and Alloin et al. (1979) [1], is usually referred to as the “strong line method” and has been widely adopted. Numerous relations (calibrations) have been proposed to convert metallicity-sensitive emission-line combinations into metallicity or temperature estimates ([9, 22, 30, 37, 38, 39, 58, 63, 64, 67], among many others). It is important to note that there are differ-

ent absolute metallicity scales in H II regions. The empirical metallicity scale is defined by the direct method (T_e method) and the empirical calibrations based on it. Metallicities derived using calibrations based on photoionisation models tend to be systematically higher (up to ~ 0.7 dex) than those derived using the direct method (see reviews in [24, 27, 28]). Therefore, there are large discrepancies between oxygen abundances in the extragalactic H II regions obtained in different works using different calibrations.

We focus on the discussion of these questions. However, we do not list and consider in details a numerous calibrations. Instead we analyse the foundations of different types of calibrations and problems which those calibrations encounter. The expressions for calibrations can be found in original papers or in the recent book [45].

Throughout the paper, we use the following standard notations for the line intensities:

$$\begin{aligned} R &= I_{[O III]\lambda 4363}/I_{H\beta}, \\ R_2 &= I_{[O II]\lambda 3727 + \lambda 3729}/I_{H\beta}, \\ N_2 &= I_{[N II]\lambda 6548 + \lambda 6584}/I_{H\beta}, \\ S_2 &= I_{[S II]\lambda 6717 + \lambda 6731}/I_{H\beta}, \\ R_3 &= I_{[O III]\lambda 4959 + \lambda 5007}/I_{H\beta}, \\ S_3 &= I_{[S III]\lambda 9068 + \lambda 9532}/I_{H\beta}, \\ R_{23} &= R_2 + R_3. \end{aligned}$$

With these definitions the excitation parameter P can be expressed as: $P = R_3/(R_2 + R_3)$. The electron temperatures is given in units of 10^4 K.

DIRECT (T_e) METHOD

The diagnostic of the physical conditions and element abundances in H II regions is based on the

*pilyugin@mao.kiev.ua

measurements of the fluxes in the emission lines [O II] λ 3727+ λ 3729, [O III] λ 4363, H β , [O III] λ 4959, [O III] λ 5007, [N II] λ 5755, [S III] λ 6312, [N II] λ 6548, H α , [N II] λ 6584, [S II] λ 6717, [S II] λ 6731, [S III] λ 9068. The hydrogen, oxygen, nitrogen and sulfur lines serve to estimate electron temperature, electron concentration, and oxygen and nitrogen abundances relative to hydrogen. The hydrogen H α and H β lines are also used to correct the emission-line fluxes for interstellar reddening using the theoretical H α to H β ratio (the standard value is H α /H β = 2.86). The analytical approximation to the Whitford interstellar reddening law can be taken from [19]. The intensities of all lines are normalised to the H β line flux. The line intensities [O III] λ 4959 and [O III] λ 5007 are required to define the R_3 value. However, only the line [O III] λ 5007 is reported in some of the papers. Therefore, the R_3 value is derived from the [O III] λ 5007 line intensity. The [O III] λ 5007 and λ 4959 lines originate from transitions from the same energy level, so their flux ratio is only due to the transition probability ratio, which is very close to 3 [62]. The measurements of the [O III] λ 5007 and λ 4959 lines in SDSS (Sloan Digital Sky Survey [66]) spectra confirm this value of the flux ratio [25]. Therefore, the value of R_3 can be estimated as $R_3 = 1.33[\text{O III}]\lambda 5007$. Similarly, the values of N_2 are estimated without the lines [N II] λ 6548. The [N II] λ 6584 and λ 6548 lines also originate from transitions from the same energy level, and the transition probability ratio for those lines is again close to 3 [62]. The value of N_2 can therefore be estimated as $N_2 = 1.33[\text{N II}]\lambda 6584$. Moreover, measurements of the [N II] λ 6584 line are more reliable than those of the [N II] λ 6548 line.

The electron density is usually estimated from the sulfur line ratio [S II] λ 6717/[S II] λ 6731. According to the five-level atom solution for the S⁺ ion, the [S II] λ 6717/[S II] λ 6731 is a reliable indicator of the electron density in the interval from $n_e \sim 10^2 \text{ cm}^{-3}$ to $n_e \sim 10^4 \text{ cm}^{-3}$ [45]. The electron density was estimated (through the density-sensitive [S II] λ 6717/[S II] λ 6731 line ratio or in other manners) in many extragalactic H II regions. It has been found that the majority of extragalactic H II regions are in low-density regime, i.e. they have a low electron density, $n_e < 100 - 200 \text{ cm}^{-3}$ [4, 15, 67]. Then the low-density approximation can be used in investigations of the extragalactic H II regions.

The standard H II region model with two distinct temperature zones within the nebula is usually adopted for determination of the oxygen and nitrogen abundances. The electron temperature within the zone O⁺⁺ is given by the electron temperature t_3 , and the temperature within the zones O⁺ and N⁺ is given by the temperature t_2 . The electron temperature t_3 is estimated from the ratio of nebular to auroral oxygen O⁺⁺ line intensities [O III](λ 4959+ λ 5007)/[O III] λ 4363 using the five-level atom solution for the O⁺⁺ ion. The electron

temperature t_2 is estimated from the ratio of nebular to auroral nitrogen N⁺ line intensities [N II](λ 6548 + λ 6584)/[N II] λ 5755 using the five-level atom solution for the N⁺ ion. In the low density regime, the simple expressions provide approximations to the numerical results with an accuracy better than 1% for both ions. It is common practice that the value of only the electron temperature is measured and the value of the other temperature is determined from the $t_2 - t_3$ relation. The $t_2 - t_3$ relation was a subject of many investigations ([7, 12, 16, 17, 20, 34, 43, 51] among many others). The $t_2 - t_3$ relation from [7, 12] is used most often.

If the near-infrared nebular sulfur line [S III] λ 9068 and auroral line [S III] λ 6312 are measured then the electron temperature $t_{3,S}$ can be derived from the ratio [S III](λ 9068 + λ 9532)/[S III] λ 6312. When the value of the electron temperature $t_{3,S}$ is measured then the value of t_3 is obtained from the relation $t_3 - t_{3,S}$ after [12].

The classic T_e method has been questioned by Peimbert [35]. It is known that metallicities derived from collisionally excited lines of heavy elements in H II regions are systematically lower than those derived from recombination lines by factors of ~ 2 ([54] and references therein). Peimbert et al. [36] have suggested that these differences can be taken into account by the presence of spatial temperature fluctuations inside H II regions. This interpretation suggests that the classic T_e method based on collisionally excited lines results in overestimated electron temperatures and, consequently, in underestimated element abundances in H II regions. However, this interpretation meets several difficulties.

First, Barlow et al. [3] have found that the recombination line abundance discrepancies appear to be restricted to ions of the second row of the periodic table (carbon, nitrogen, oxygen, and neon), but do not affect third row ions (e.g. magnesium). Nebular temperature fluctuations cannot account for this fact.

Second, Guseva et al. [13, 14] have determined for a large sample of H II regions the temperatures $T_e(\text{H}^+)$ of the H⁺ zones using the Balmer and Paschen jumps, and the temperatures $T_e([\text{O III}])$ of the O⁺⁺ zones from collisionally excited lines. They found that the $T_e(\text{H}^+)$ and $T_e([\text{O III}])$ temperatures do not differ statistically, although small temperature differences of the order of 3–5% cannot be ruled out.

Third, the interstellar oxygen abundance in the solar vicinity, derived with very high precision from the high-resolution observations of the weak interstellar O I λ 1356 absorption line towards the stars is model-independent and can serve as a “Rosetta Stone” to make a choice between “theoretical” and “empirical” scales of oxygen abundances in high-metallicity H II regions. The agreement between the value of the oxygen abundance at the solar galacto-

centric distance traced by the abundances derived in H II regions through the T_e method and that derived from the interstellar absorption lines towards the stars is strong evidence that the classical T_e method provides accurate oxygen abundances in H II regions, i.e. the “empirical” scale of oxygen abundances in high-metallicity H II regions is correct (see discussion and references in [41]). Thus, oxygen abundances derived with the T_e method have been verified by high-precision model-independent determinations of the interstellar oxygen abundance in the solar vicinity. More recently, Williams et al. [65] have measured UV resonance line absorptions in the spectra of central stars of planetary nebulae produced by the nebular gas, for the ions that emit optical forbidden lines. They found that the collisionally excited forbidden lines yield column densities that are in basic agreement with the column densities derived for the same ions from the UV absorption lines. Williams et al. [65] have concluded that the temperatures and abundances based on the forbidden lines are reliable.

Fourth, Bresolin et al. [6] have shown that the oxygen abundances derived with the T_e method in H II regions of the spiral galaxy NGC 300 agree well with the stellar abundances. They have concluded that the T_e -based chemical abundances in extragalactic H II regions are reliable measures of the nebular abundances.

The discrepancies between metallicities based on the collisionally excited lines and those based on the recombination lines can be caused by errors in the line recombination coefficients by factors of ~ 2 [54].

Thus, there are strong evidences that the metallicity scale defined by the classic T_e method is the most reliable one. The equations relating ion abundances to measured line fluxes and electron temperatures (e.g. $12 + \log(\text{O}^+/\text{H}^+) = f(R_2, t_2)$) are derived through the approximations to the numerical results for the five-level atom solution for the corresponding ion. As a new atomic data appear the equations relating electron temperatures to measured line fluxes as well the equations relating ion abundances to measured line fluxes and electron temperatures are updated through the five-level atom solutions for the new atomic data. The error in the electron temperature due to uncertainties in the atomic data (in Einstein coefficients for spontaneous transitions and in effective collision strengths for electron impacts) increases with electron temperature. At temperature 10000 K, the error in the electron temperature ($t_{3,\text{O}}$ and $t_{2,\text{N}}$) is not in excess of several per cents [44, 49]. The uncertainties in atomic data were estimated as a discrepancy between values computed by different authors.

The expressions for the recent atomic data (and the comparison to the previous expressions) can be found in [45].

STRONG LINE METHOD: CALIBRATIONS FUNDAMENTAL SEQUENCE OF H II REGIONS

The emission line properties of photoionized H II regions are governed by its heavy element content and by the electron temperature distribution within the photoionized nebula. In turn, the latter is controlled by the ionizing star cluster spectral energy distribution and by the chemical composition of the H II region. The evolution of a giant extragalactic H II region associated with a star cluster is thus caused by a gradual change in time of the integrated stellar energy distribution due to stellar evolution. This has been the subject of numerous investigations ([9, 10, 29, 31, 32, 55, 56, 60], among others). The general conclusion from those studies is that H II regions ionized by star clusters form a well-defined fundamental sequence in different emission-line diagnostic diagrams. The existence of such a fundamental sequence forms the basis of various investigations of extragalactic H II regions.

First, Baldwin et al. [2] have suggested that the position of an object in some well-chosen emission-line diagrams can be used to separate H II regions ionized by star clusters from other types of emission-line objects. This idea has found general acceptance and use. Thus, the $[\text{O III}]\lambda 5007/\text{H}\beta$ vs $[\text{N II}]\lambda 6584/\text{H}\alpha$ diagram has been used widely to distinguish between star-forming galaxies and active galactic nuclei (AGNs). In particular, the SDSS emission-line galaxies occupy a well-defined region shaped like the wings of a seagull [61]. The left wing consists of star-forming galaxies while the right wing is attributed to AGNs (see Fig. 1). However, the exact location of the dividing line between H II regions and AGNs is still controversial [21, 23, 59]. The objects that lie between the dividing lines according to Kauffmann et al. [21] and Kewley et al. [23] in the $[\text{N II}]\lambda 6584/\text{H}\alpha$ versus $[\text{O III}]\lambda 5007/\text{H}\beta$ diagram (Fig. 1) are starburst like objects if the dividing line according to [23] is used but they are AGN-like objects (or, at least, they are not purely thermally photoionised objects) if the dividing line according to [21] is used. The dividing line suggested by Stasińska et al. [59] is close to that from [21]. It has been argued [53] that the line according to [21] is to be favoured as it outlines the area occupied by certainly starburst-like objects in the $[\text{O III}]\lambda 5007/\text{H}\beta$ vs. $[\text{N II}]\lambda 6584/\text{H}\alpha$ diagram.

Second, Pagel et al. [33] and Alloin et al. [1] have suggested that the positions of H II regions in some emission-line diagrams can be calibrated in terms of their oxygen abundances. This approach to abundance determination in H II regions, usually referred to as the “strong line method” has been widely adopted, especially in cases where the temperature-sensitive $[\text{O III}]\lambda 4363$ line is not detected. McGaugh [30] advocated the idea that the strong oxygen lines ($[\text{O II}]\lambda 3727 + \lambda 3729$, $[\text{O III}]\lambda 4959 + 5007$) contain the

necessary information for determination of accurate oxygen abundances in low metallicity H II regions. It has been found empirically that there exists a relation (the ff relation) between auroral [O III] λ 4363 and nebular oxygen line fluxes in spectra of H II regions [42]. The ff relation allows one to estimate the flux in the auroral line from strong oxygen line measurements only. This solves the problem of the electron temperature (and, consequently, abundance) determination in H II regions. The ff relation confirms the basic idea of the strong line method that the oxygen abundance in H II region can be estimated from the strong oxygen lines measurements only. It is interesting to note that the realisation of the classic T_e method in practice is also based on the existence of the fundamental sequence of H II regions. Indeed, when only one electron temperature, t_3 or t_2 , is measured it is standard practice to use a $t_2 - t_3$ relation to estimate the other temperature. This relation is usually established on the basis of H II regions models which belong to the same fundamental sequence.

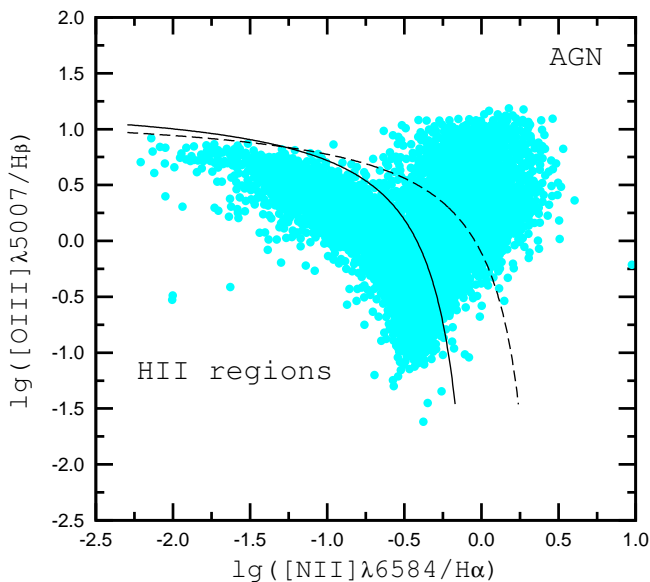


Fig. 1: The [N II] λ 6584/H α versus [O III] λ 5007/H β diagram. The grey points are SDSS objects. The solid line separates objects with H II spectra from those containing an AGN according to Kauffmann et al. [21], while the dashed line is the same according to Kewley et al. [23].

Numerous relations have been suggested to convert metallicity-sensitive emission-line ratios into metallicity or temperature estimates (e. g. [5, 8, 9, 11, 22, 26, 29, 37, 38, 39, 48, 50, 52, 58, 63, 64, 67]). Relation of this kind is usually named calibration since some metallicity indicator (combination of the strong line intensities in the spectra) for H II regions is calibrated in terms of their oxygen abun-

dances. There is a good correlation between oxygen abundance and electron temperature in H II regions (see Fig. 2). Therefore, a reliable temperature index should also be a reliable metallicity index.

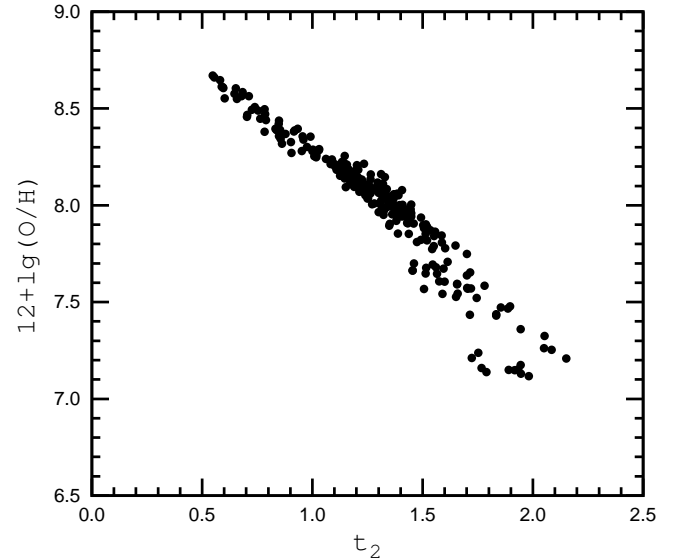


Fig. 2: Oxygen abundance O/H as a function of electron temperature t_2 for the sample of well-measured H II regions.

It should be emphasised that there are two different absolute O/H scales. The empirical metallicity scale is defined by H II regions with abundances derived through the direct method (T_e method). The theoretical (or model) metallicity scale is defined by the set of photoionisation models of H II regions. As consequence, there are two types of calibrations: 1) theoretical (or model) calibrations based on photoionization models, and 2) empirical calibrations based on H II regions with measured electron temperatures. Metallicities derived using calibrations based on photoionisation models tend to be systematically higher (up to ~ 0.7 dex) than those derived using the direct method [24, 27, 28, 41]. Because of the large abundance discrepancies between the different types of calibrations, the question then arises: which type of calibration is the most reliable? Stasińska [57] has noted that “a widespread opinion is that photoionization model fitting provides the most accurate abundances. This would be true if the constraints were sufficiently numerous (not only on emission line ratios, but also on the stellar content and on the nebular gas distribution) and if the model fit were perfect (with a photoionization code treating correctly all the relevant physical processes and using accurate atomic data). These conditions are never met in practice”. Thus, the statement that H II region models provide realistic abundances should not be taken for granted. On the other hand, it was argued above that the classic T_e method produces realistic

temperatures and abundances in H II region. Thus, there are strong evidences that the metallicity scale defined by the H II regions with abundances determined through the classic T_e method is the most reliable one.

R_{23} CALIBRATIONS

The oxygen abundance indicator $R_{23} = ([\text{O II}]\lambda\lambda 3727, 3729 + [\text{O III}]\lambda\lambda 4959, 5007)/\text{H}\beta$, suggested by Pagel et al. [33], has found widespread acceptance and use for the oxygen abundance determination in H II regions where the temperature-sensitive lines are undetectable. The early R_{23} calibrations were one-dimensional, i.e. a relation of the type $\text{O}/\text{H} = f(R_{23})$ was used. Different $\text{O}/\text{H} = f(R_{23})$ expressions have been suggested using different sets of photoionisation models of H II regions as a calibration data points [9, 11, 29, 64, 67]. Each calibration produces the abundances in the metallicity scale defined by calibration data points. Fig. 3 shows R_{23} calibrations after [11] (solid line) and after [64] (dashed line) superimposed on the T_e -based abundances in H II regions (grey points). Inspection of Fig. 3 shows that theoretical R_{23} calibrations provide more or less realistic oxygen abundances in low-metallicity H II regions, but yields overestimated oxygen abundances in high-metallicity H II regions.

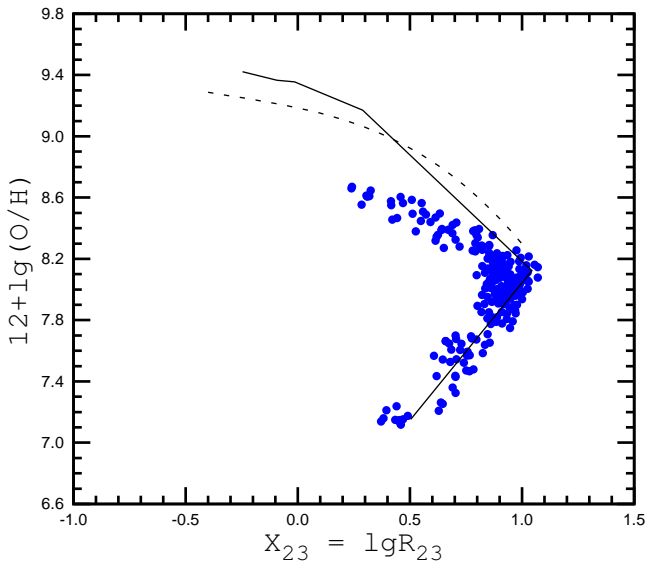


Fig. 3: The $R_{23} - \text{O}/\text{H}$ diagram. The R_{23} calibrations after Edmunds & Pagel (1984) [11] (solid line) and after Tremonti et al. (2004) [64] (dashed line) superimposed on the T_e -based abundances in H II regions (grey points).

All R_{23} calibrations (empirical as well as theoretical) encounter problems. *First*. It is well known that the relation between the oxygen abundance and the strong oxygen line intensities is double-valued, with two distinct parts traditionally known as the upper and lower branches of the $R_{23} - \text{O}/\text{H}$ diagram

(see Fig. 3). Two distinct relations between the oxygen abundance and the strong oxygen line intensities should be established, one for the upper branch (the high-metallicity calibration) and one for the lower branch (the low-metallicity calibration). The expression for the oxygen abundance determination in high metallicity H II regions is valid only for H II regions that belong to the upper branch. Thus, one has to know *a priori* on which of the two branches the H II region lies. An unjustified use of expression for the oxygen abundance determination in high metallicity H II regions in the determination of the oxygen abundance in low-metallicity H II regions would result in overestimated oxygen abundances [40]. Moreover, the strong oxygen-line intensities are not a good indicator of the oxygen abundance in the transition zone between the upper and lower branches.

Second. It has been shown [38, 39, 50] that the error in the oxygen abundance derived with the one-dimensional calibrations involves a systematic error. The origin of this systematic error is evident. In a general case, the intensity of oxygen emission lines in spectra of H II regions depends not only on the oxygen abundance but also on the physical conditions (hardness of the ionizing radiation and geometrical factors) in the ionized gas. Thus, when one estimates the oxygen abundance from emission line intensities, the physical conditions in H II regions should be taken into account. In the T_e method this is done via the electron temperature T_e . In one-dimensional calibrations the physical conditions in H II regions are ignored.

It has been shown [38, 39, 50] that the physical conditions in H II regions can be estimated and taken into account via the excitation parameter P . A two-dimensional or parametric empirical calibration (the so-called “P method”) has been suggested. A more general relation of the type $\text{O}/\text{H} = f(P, R_{23})$ is used in the P method, compared with the relation of the type $\text{O}/\text{H} = f(R_{23})$ used in one-dimensional calibrations. The two-dimensional theoretical R_{23} calibrations were suggested by Kobulnicky et al. [26] and Kewley & Dopita [22].

The theoretical calibration of Kobulnicky et al. agrees quantitatively with the recent oxygen abundances derived through the direct method (the T_e method) at low metallicities. The discrepancy between the theoretical calibration from [26] and the empirical calibration from [38, 39] is negligible small for the very low-metallicity ($12 + \log\text{O}/\text{H}$ around 7.3), high-excitation (P around 0.95) H II regions, but discrepancy increases with the increasing of the metallicity and with the decreasing of the excitation parameter, reaching the value of $\Delta \log\text{O}/\text{H}$ around 0.15 dex for H II regions with $12 + \log\text{O}/\text{H}$ around 7.9. The agreement between the two-dimensional theoretical R_{23} calibration and the empirical calibration disappears for H II regions which lie on the upper branch of the $\text{O}/\text{H} - R_{23}$ diagram. It should be

noted that there is a significant discrepancy between two-dimensional theoretical calibration from [22] and that from [26] both at high and low metallicities.

ANOTHER ABUNDANCE INDICATORS

The main problem of the R_{23} index is that it is double valued. Therefore another index is needed to decide whether one has to choose the low-metallicity or the high-metallicity solution. Different combinations of the strong lines of oxygen, nitrogen and sulfur (and other elements) have been proposed as metallicity (temperature) indices. Ideally, one would require from a metallicity index to: (i) be single valued with respect to metallicity, (ii) have a behaviour dominated by a well understood “physical” reason, (iii) be unaffected by the presence of diffuse ionized gas, and (iv) be independent of chemical evolution [58].

Fig. 4 shows how the fluxes and flux ratios of various strong emission lines in well-studied (calibrating) H II regions vary as a function of oxygen abundance. Inspection of those variations shows that none of the considered emission line fluxes and flux ratios displays a monotonic behaviour with oxygen abundance over the whole metallicity range. Instead, the sequences show bends. Those properties prevent the construction of a calibration that works over the whole range of metallicities shown by H II regions. Thus, one has to construct separate calibrations for different metallicity intervals, i. e., there are no calibration relations that work sufficiently well over the whole range of observed metallicities. Here, also another problem arises – one has to know *a priori* in which metallicity interval (or on which of the two branches) the H II region is located.

In the cool high-metallicity H II regions, the R_2 and R_3 line fluxes strongly decrease with increasing oxygen abundance. On the contrary, the N_2 line fluxes increase with oxygen abundance. The behaviour difference between the R_2 and N_2 line fluxes have a natural explanation as the interplay of two factors. On the one hand, the line-emissivity $j(R_2)$ is temperature sensitive, i. e. the emissivity decreases with decreasing electron temperature, causing a decrease of the R_2 line flux for lower electron temperatures. On the other hand, the oxygen abundance increases on average with decreasing electron temperature, resulting in an increase of the R_2 line flux with decreasing electron temperature. The combination of these two factors results in a decrease of the R_2 line flux with decreasing of electron temperature. Since at $12 + \log(\text{O}/\text{H}) > 8.3$, secondary nitrogen becomes dominant and the nitrogen abundance increases at a faster rate than the oxygen abundance [18], then the change of nitrogen abundances with decreasing electron temperature is larger than that of oxygen abundances and, as a consequence, compensates the decrease of the line-emissivity $j(N_2)$. Thus, the N_2 line fluxes increase with oxygen abundance. One can thus expect the N_2 parameter to act

as surrogate metallicity index.

The energy of the level that gives rise to the R_2 line (the [O II]($\lambda 3727 + \lambda 3729$) doublet) is higher than both the energies of the levels giving rise to the S_2 and N_2 lines. Thus, the line-emissivity ratios $j(N_2)/j(R_2)$ and $j(S_2)/j(R_2)$ are temperature sensitive: they increase with decreasing electron temperature. It should be noted however that these line ratios are not exclusively governed by the dependence of the line-emissivities on the electron temperature. In the case of sulfur, one may assume that the S/O abundance ratio is constant in all H II regions, since sulfur and oxygen are thought to be produced by the same massive stars. However, the S^+ zone does not coincide with the O^+ zone [12], and their size ratio is thought to depend on the electron temperature. One can then expect that, to first approximation, the S_2/R_2 ratio depends only on the electron temperature. It can then be used as a surrogate indicator of the electron temperature (metallicity), although the temperature dependence of $S_2/R_2 = f(t_2)$ is more complex than that of $j(S_2)/j(R_2) = f(t_2)$. In the case of nitrogen, the N^+ zone is nearly coincident with the O^+ zone [12]. But the N/O abundance ratio is not the same for all H II regions. At high metallicities, the N/O abundance ratio increases with decreasing electron temperature (i. e. with increasing oxygen abundance) [18]. Again, one can expect that, to first approximation, the N_2/R_2 ratio depends only on electron temperature and can be used as a surrogate indicator of the electron temperature (metallicity), although the temperature dependence $N_2/R_2 = f(t_2)$ is also more complex than that of $j(N_2)/j(R_2) = f(t_2)$. One can thus expect that both N_2/R_2 and S_2/R_2 ratios are surrogate temperature (metallicity) indices.

Calibrations based on oxygen, nitrogen and sulfur strong lines have been considered in a number of studies ([5, 8, 37, 48, 52, 58, 63], among many others). It is common practice, in constructing the calibration, to establish relations between the oxygen abundances and the strong-line fluxes. Thuan et al. [63] have calibrated the positions of H II regions in three different diagnostic diagrams in terms of nitrogen abundances and electron temperatures. The oxygen abundance can then be estimated from the obtained nitrogen abundance and the N/O ratio. It has been shown that, by using calibrations based on several indices, the accuracy of abundance estimates can be significantly improved [48, 52]. The discussion of different calibrations can be found in [45].

THE COUNTERPART METHOD

Each existing calibration is based on the assumption that H II regions with similar strong-line intensities have similar abundances. A simple, more direct method for abundance determination follows from that assumption as well [47]. If there were (and fortunately there is indeed) a suitable sample

of reference H II regions with well-measured electron temperatures and abundances, then one can choose among those reference H II regions the ones that have the smallest difference in strong line intensities compared to the studied H II region, i. e., one can find a corresponding “counterpart” (or “twin”) H II region. Then the oxygen and nitrogen abundances and electron temperatures in the investigated H II region can be assumed to be the same as in its counterpart. In other words, the abundances in the target H II region can be determined “by precedent”. To obtain more reliable abundances, one may select several reference H II regions (counterparts) and then estimate the abundance in the target H II region through extrapolation or interpolation. We will refer to this method as the “counterpart method” or, for brevity, as the *C* method.

To find the counterpart for the H II region under study, it is preferable to compare not the measured nebular lines R_3 , R_2 , N_2 , and S_2 directly, but instead other values that are expressed in terms of these line intensities: $P = R_3/(R_2 + R_3)$ (excitation parameter), $\log R_3$, $\log(N_2/R_2)$, and $\log(S_2/R_2)$. A linear combination of these values can serve as an indicator of the metallicity in an H II region [52]. A counterpart for the considered H II region can be chosen by comparison of four combinations of strong-line intensities (P , $\log R_3$, $\log(N_2/R_2)$, and $\log(S_2/R_2)$) in [47]. The *C* method has been modified in [46]. To find the counterpart for the H II region under study, it is suggested to compare not the four values that are expressed in terms of the strong line intensities but two sets of three values: 1) $\log R_3$, P and $\log(N_2/R_2)$ and 2) $\log R_3$, $\log N_2$ and $\log(N_2/S_2)$. The *C*-based (obtained using the *C* method) abundances in a large sample of H II regions in nearby irregular and spiral galaxies were estimated in [46].

The *C* method requires a sample of reference H II regions, i. e. a sample of H II regions with reliable abundances. The sample of reference H II regions can be selected among H II regions in irregular and spiral galaxies with T_e -based abundances (with measured electron temperatures). The selection of reference H II regions is not a trivial task. One may select reference H II regions where the discrepancies between the *C*-based and the T_e -based oxygen and nitrogen abundances are less than a fixed value [47, 46]. The sample of reference H II regions in [46] contains 250 objects. This sample (*E2013*, etalon sample 2013) are shown in Fig. 2, Fig. 3, and Fig. 4.

CONCLUDING REMARKS

Spectroscopic measurements of H II regions in nearby galaxies were carried out in many works (e. g. see list of references in [46]). The H II regions in one or several galaxies are usually measured and the element abundances are estimated. The different methods for abundance determinations are used in different works. As a result, the abundances from different

works are not homogeneous and cannot be directly compared to each other. Therefore, the abundances from different works can be compared and analysed only after those abundances are homogenised, i. e., all the abundances are redetermined in a uniform way.

The empirical metallicity scale has advantages as compared to the theoretical (model) metallicity scales. The empirical metallicity scale is well defined in terms of the abundances in H II regions derived through the classic T_e method, i. e., in that sense the empirical metallicity scale is absolute. The abundances estimated via different empirical calibrations are compatible with each other and with the T_e -based abundances as well. Contrary to the consistency among empirical calibrations, there are as many theoretical (model) metallicity scales as there are sets of H II region models. In other words, the abundances derived using different theoretical calibrations are usually not in agreement with each other. Thus, the empirical metallicity scale is likely the preferable metallicity scale at present.

It should be noted that the calibrations cannot be used for the abundance determinations in H II regions in our Galaxy. It was emphasised above that the H II regions ionized by star clusters form a well-defined fundamental sequence in different emission-line diagnostic diagrams and the existence of such a fundamental sequence forms the basis of various calibrations. High-precision spectroscopy a number of H II regions in our Galaxy has been carried out. However, only a small part of the H II regions is measured in these cases and therefore the obtained line intensities are usually not representative for the whole nebula. For this reason, these spectroscopic measurements cannot be used in abundance determinations through the calibrations.

REFERENCES

- [1] Alloin D., Collin-Souffrin S., Joly M. & Vigroux L. 1979, A&A, 78, 200
- [2] Baldwin J. A., Phillips M. M. & Terlevich R. 1981, PASP, 93, 5
- [3] Barlow M. J., Liu X.-W., Péquignot D. et al. 2003, IAU Symposium 209, 373
- [4] Bresolin F., Schaerer D., González Delgado R. M. & Stasińska G. 2005, A&A, 441, 981
- [5] Bresolin F. 2007, ApJ, 656, 186
- [6] Bresolin F., Gieren W., Kudritzki R.-P. et al. 2009, ApJ, 700, 309
- [7] Campbell A., Terlevich R. & Melnick J. 1986, MNRAS, 223, 811
- [8] Denicoló G. Terlevich R. & Terlevich E. 2002, MNRAS, 330, 69
- [9] Dopita M. A. & Evans I. N. 1986, ApJ, 307, 431
- [10] Dopita M. A., Fischera J., Sutherland R. S. et al. 2006, ApJS, 167, 177
- [11] Edmunds M. G. & Pagel B. E. J. 1984, MNRAS, 211, 507
- [12] Garnett D. R. 1992, AJ, 103, 1330

- [13] Guseva N. G., Izotov Y. I., Papaderos P. & Fricke K. J. 2007, A&A, 464, 885
- [14] Guseva N. G., Izotov Y. I. & Thuan T. X. 2006, ApJ, 644, 890
- [15] Gutiérrez L. & Beckman J. E. 2010, ApJ, 710, L44
- [16] Hägele G. F., Díaz Á. I., Terlevich E. et al., 2008, MNRAS, 383, 209
- [17] Hägele G. F., Pérez-Montero E., Díaz Á. I., Terlevich E. & Terlevich R. 2006, MNRAS, 372, 293
- [18] Henry R. B. C., Edmunds M. G. & Köppen J. 2000, ApJ, 541, 660
- [19] Izotov Y. I., Thuan T. X. & Lipovetsky V. A. 1994, ApJ, 435, 647
- [20] Izotov Y. I., Thuan T. X. & Lipovetsky V. A. 1997, ApJS, 108, 1
- [21] Kauffmann G., Heckman T. M., Tremonti C. et al. 2003, MNRAS, 346, 1055
- [22] Kewley L. J. & Dopita M. A. 2002, ApJS, 142, 35
- [23] Kewley L. J., Dopita M. A., Sutherland R. S., Heisler C. A. & Trevena J. 2001, ApJ, 556, 121
- [24] Kewley L. J. & Ellison S. L. 2008, ApJ, 681, 1183
- [25] Kniazev A. Y., Pustilnik S. A., Grebel E. K., Lee H. & Pramskij A. G. 2004, ApJS, 153, 429
- [26] Kobulnicky H. A., Kennicutt R. C., Jr. & Pizagno J. L. 1999, ApJ, 514, 544
- [27] López-Sánchez Á. R., Dopita M. A., Kewley L. J. et al. 2012, MNRAS, 426, 2630
- [28] López-Sánchez Á. R. & Esteban C. 2010, A&A, 517, 85
- [29] McCall M. L., Rybski P. M. & Shields G. A. 1985, ApJS, 57, 1
- [30] McGaugh S. S. 1991, ApJ, 380, 140
- [31] Melekh B. Ya., Pilyugin L. S. & Korytko R. I. 2012, Kinematics and Physics of Celestial Bodies, 28, 4, 189
- [32] Moy E., Rocca-Volmerange B. & Fioc M. 2001, A&A, 365, 347
- [33] Pagel B. E. J., Edmunds M. G., Blackwell D. E., Chun M. S. & Smith G. 1979, MNRAS, 189, 95
- [34] Pagel B. E. J., Simonson E. A., Terlevich R. J. & Edmunds M. G. 1992, MNRAS, 255, 325
- [35] Peimbert M. 1967, ApJ, 150, 825
- [36] Peimbert M., Storey P. J. & Torres-Peimbert S. 1993, ApJ, 414, 626
- [37] Pettini M. & Pagel B. E. J. 2004, MNRAS, 348, L59
- [38] Pilyugin L. S. 2000, A&A, 362, 325
- [39] Pilyugin L. S. 2001, A&A, 369, 594
- [40] Pilyugin L. S. 2003, A&A, 397, 109
- [41] Pilyugin L. S. 2003, A&A, 399, 1003
- [42] Pilyugin L. S. 2005, A&A, 436, L1
- [43] Pilyugin L. S. 2007, MNRAS, 375, 685
- [44] Pilyugin L. S. 2010, Kinematika i Fizika Nebesnykh Tel, 20, 2, 3
- [45] Pilyugin L. S. 2013, 'Ionized gas in galaxies: physical conditions and chemical composition', Naukova Dumka, Kiev
- [46] Pilyugin L. S., Grebel E. K. & Kniazev A. Y. 2013, MNRAS, submitted
- [47] Pilyugin L. S., Grebel E. K. & Mattsson L. 2012, MNRAS, 424, 2316
- [48] Pilyugin L. S. & Mattsson L. 2011, MNRAS, 412, 1145
- [49] Pilyugin L. S., Mattsson L., Vílchez J. M. & Cedrés B. 2009, MNRAS, 398, 485
- [50] Pilyugin L. S. & Thuan T. X. 2005, ApJ, 631, 231
- [51] Pilyugin L. S., Vílchez J. M. & Thuan T. X. 2006, MNRAS, 370, 1928
- [52] Pilyugin L. S., Vílchez J. M. & Thuan T. X. 2010, ApJ, 720, 1738
- [53] Pilyugin L. S., Zinchenko I. A., Cedrés B. et al. 2012, MNRAS, 419, 490
- [54] Rodríguez M. & García-Rojas J. 2010, ApJ, 708, 1551
- [55] Stasińska G. 1978, A&A, 66, 257
- [56] Stasińska G. 1980, A&A, 84, 320
- [57] Stasińska G. 2004, in *Cosmochemistry. The melting pot of the elements. XIII Canary Islands Winter School of Astrophysics, Puerto de la Cruz, Tenerife, Spain, November 19-30, 2001*, eds.: Esteban C., Garcá López R. J., Herrero A., Sánchez F., Cambridge University Press, Cambridge, 115
- [58] Stasińska G., 2006, A&A, 454, L127
- [59] Stasińska G., Cid Fernandes R., Mateus A., Sodré L. & Asari N. V. 2006, MNRAS, 371, 972
- [60] Stasińska G. & Izotov Y. 2003, A&A, 397, 71
- [61] Stasińska G., Vale Asari N., Cid Fernandes R. et al. 2008, MNRAS, 391, L29
- [62] Storey P. J. & Zeppen C. J. 2000, MNRAS, 312, 813
- [63] Thuan T. X., Pilyugin L. S. & Zinchenko I. A. 2010, ApJ, 712, 1029
- [64] Tremonti C. A., Heckman T. M., Kauffmann G. et al. 2004, ApJ, 613, 898
- [65] Williams R., Jenkins E. B., Baldwin J. A. et al., 2008, ApJ, 677, 1100
- [66] York D. G., Adelman J., Anderson J. E., Jr. et al. 2000, AJ, 120, 1579
- [67] Zaritsky D., Kennicutt R. C., Jr. & Huchra J. P. 1994, ApJ, 420, 87

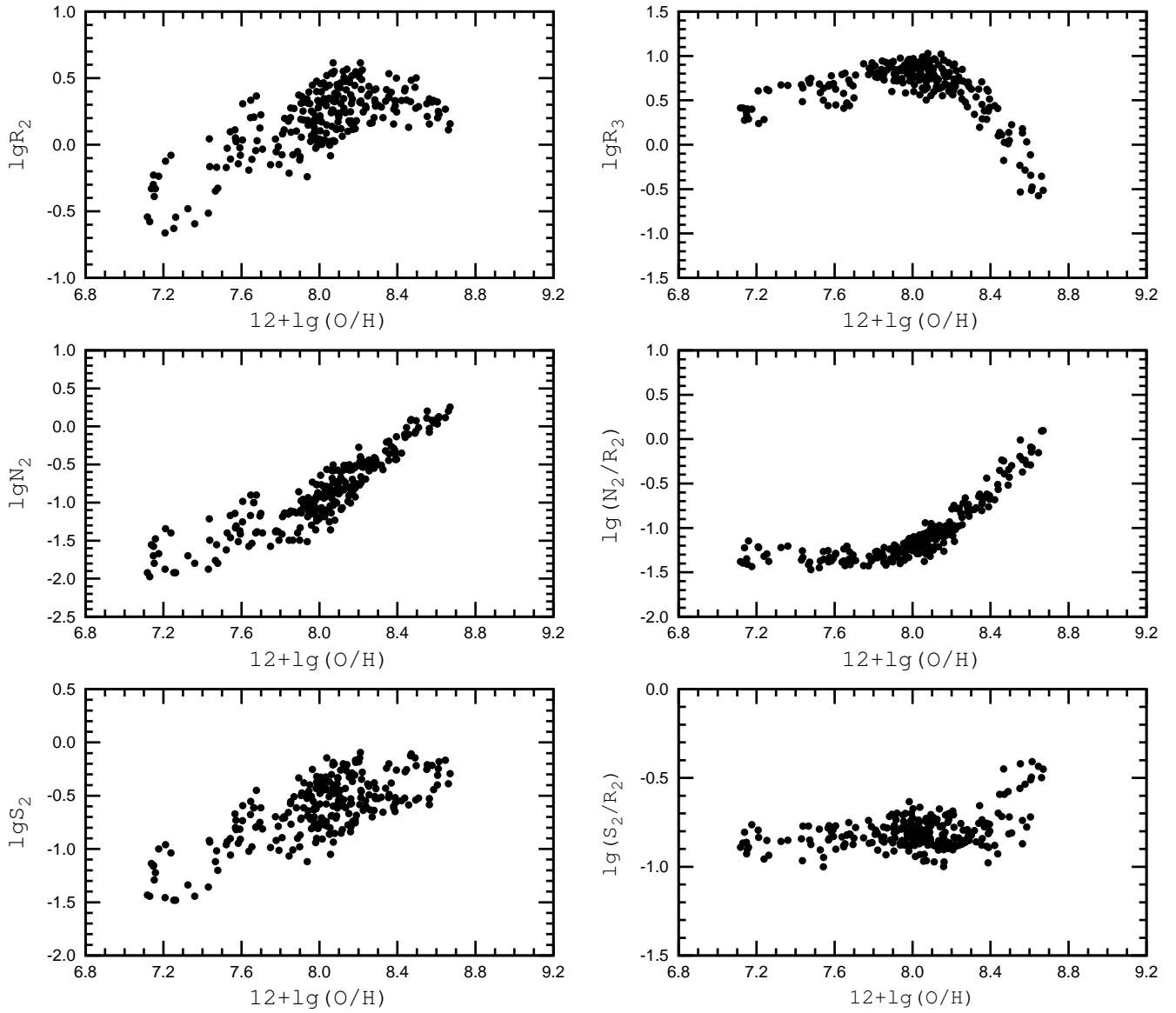


Fig. 4: Emission line fluxes and line flux ratios as a function of oxygen abundance $12 + \log(\text{O}/\text{H})$ for the sample of well-measured H II regions.